Full paper / Mémoire

One-pot microwave-assisted green synthesis of amine-functionalized graphene quantum dots for high visible light photocatalytic application

Tran Van Tam [a], [**], T.M. Altahtamouni [b], Vien Le Minh [c], Huynh Ky Phuong Ha [c], Nguyen Thi Kim Chung [d], Doan Van Thuan [e], [*]

[a] *School of Chemical Engineering, University of Ulsan, 93 Daehak-ro Nam-gu, Ulsan, 680-749, Republic of Korea*
[b] *Materials Science and Technology Program, College of Arts and Sciences, Qatar University, Doha, 2713, Qatar*
[c] *Faculty of Chemical Engineering, Ho Chi Minh City University of Technology, VNU-HCM, Ho Chi Minh City, 700000, Viet Nam*
[d] *Department of Physics, Thu Dau Mot University, 6 Tran Van on Street, Thu Dau Mot City, 820000, Binh Duong Province, Viet Nam*
[e] *NTT Institute of High Technology, Nguyen Tat Thanh University, 300a Nguyen Tat Thanh Street, Dictrict 4, Ho Chi Minh City, Viet Nam*

ARTICLE INFO

ABSTRACT

Nowadays, graphene quantum dots (GQDs) have gained a huge interest in the field of visible-range photocatalysts because of their tunable band gap and stable photochemical properties. In this work, amine-functionalized GQDs (AGQDs) were successfully prepared by one-step microwave-assisted conversion of glucose, H_2O_2, and NH_3 solution. The obtained quantum dots possess the high quality of graphene structure with the average size of 3.78 nm as well as exhibit a strong green fluorescence with a high quantum yield. Interestingly, the amine-functionalized dots perform outstanding visible-light absorption. To further investigate photocatalytic properties, a composite of AGQDs and TiO_2 was then prepared by a simple mixing route. The hybrid material showed high catalytic activity of dye degradation under visible light irradiation, which indicates the key role of AGQDs in enhancing light absorption and induced electron−hole separation. The current study may open a new way for construction of effective visible light photocatalytic systems with a cost-effective, simple approach.

© 2019 Académie des sciences. Published by Elsevier Masson SAS. All rights reserved.

1. Introduction

Over the past decades, great effort has been devoted to generating new classes of quantum dots (QDs) for substituting traditional semiconductor nanostructures containing toxic and hazardous heavy metals that have adverse impacts on human health and environment. As a rising star among the family of QDs, graphene quantum dots (GQDs) have drawn much interest in both theoretical and experimental research owing to their controllable optical properties that are originated from quantum confinement and edge effects [1,2]. In comparison to heavy-metal-containing QDs, GQDs present many superior characterics, such as biocompatibility, low cytotoxicity, environmental friendliness, good solubility, high stability, and stable luminescence against photobleaching and blinking [3−6]. Thus, the GQDs hold great promise for applications in bioimaging, photovoltaic and optoelectronic devices, and fluorescent probes [7−9]. Recently, two main methods have been developed to synthesize GQDs which are top-down and bottom-up methods. The first approach is based on breaking graphene sheets or carbon-based materials into GQDs through physical or chemical

 * Corresponding author.
 ** Corresponding author.
 E-mail addresses: tranvantamvn1989@gmail.com (T. Van Tam), doanthuanms@gmail.com (D. Van Thuan).

treatment [9]. However, the top-down method is impeded in practical applications because of the low-yield production and harmful synthetic process requiring the use of strong oxidation and organic substances [2,10-12]. On the other hand, the bottom-up strategies generate GQDs by carbonizing small hydrocarbon molecules under catalytic or thermal reactions, offering a simple and green way to prepare high-quality GQDs with a large-scale product [13, 14]. Recent research mostly has been directed at studying optical properties and synthetic strategy of GQDs, but analytical applications based on their fluorescent properties are still unfulfilled. There is a demand for developing GQDs with a high quantum yield as well as excellent selectivity and sensitivity for specific analytes.

TiO$_2$ as a traditional photocatalyst also has been widely used because of its high surface hydrophilicity and ability to decompose organic pollutants through photocatalytic processes. However, TiO$_2$-based substances currently have a challenge of low catalytic performances under visible light because of its wide band gap (3.2 eV) [15–18]. GQDs, which can tailor the band structure through functionalization, possess excellent visible light photocatalysis as well as low-cost and simple synthetic process that makes it become the most attractive material in the field of photocatalytic environmental purification. Additionally, the GQDs can enhance separation of photoinduced charge carriers in heterostructures. According to many reports, GQDs combined with TiO$_2$ nanostructures can effectively improve charge separation performance, thus leading to boost photocatalytic activity of the composite.

Herein, we have demonstrated a facile, green, and one-step synthesis of amine-functionalized GQDs (AGQDs) through one-step microwave-assisted carbonization of glucose in the presence of ammonia and H$_2$O$_2$. Without the use of a strong acid, oxidant, and other chemical reagent, AGQDs were prepared in an aqueous solution, implying that the process proposed here is relatively simple and environmentally friendly. The AGQDs obtained here possess a uniform size distribution of 3–4 nm with a thickness of a few graphene layers, and the primary amine groups were successfully functionalized onto the surface of graphene quantum dots. Moreover, the prepared AGQDs show a high quantum yield (39%) with strong green emission, resulting from electronic structure change by the successful introduction of amine-containing groups. Based on these features of the prepared GQDs, we have also developed a novel composite of AGQDs and commercial TiO$_2$ (P25) for effective visible light photocatalysts.

2. Experimental section

2.1. Materials

Glucose (99) and ammonia solution (30 wt% in water) and H$_2$O$_2$ (25%) were purchased from Sigma-Aldrich. All chemicals and solvents were used as received without any further purification. Deionized water (DI) produced by a Milli-Q Millipore system (18.2 MΩ, Millipore Corp., Billerica, MA) was used in all the experiments.

2.2. Synthesis of amine-functionalized graphene quantum dots

The AGQDs were synthesized by carbonization of glucose (99%, Sigma-Aldrich) with ammonia (30%) and H$_2$O$_2$ (25%) through a microwave-assisted approach. The synthetic procedure is a modification of a previously reported method [19]. In brief, 4 mL of a glucose transparent solution (4 mg/mL), 1 mL of ammonia, and 0.5 mL of H$_2$O$_2$ were added together and stirred for 30 min in a vial. Then, the mixture was treated for 4 min in a microwave oven (Preekem Scientific Instrument Co. Ltd.) with the operating power of 700 W. After the solution was naturally cooled down to room temperature, the obtained solution was filtered through a Teflon membrane of 0.22 μm. The final yellow light solution was dialyzed in dialysis tubing (3000 Da, Spectrum Lab. Inc.) against DI water for 1 day to remove impurities and unreacted H$_2$O$_2$ and ammonia. Finally, an aqueous AGQDs solution was collected. For the synthesis of GQDs, a similar process was employed without an ammonia and H$_2$O$_2$ solution.

2.3. Preparation of AGQDs and TiO$_2$ composite

Typically, 30 mg of commercial P25 was added into 50 ml of AGQD solution (0.05 mg/ml). The solution was sonicated for 1 h and then kept stirring for 24 h. The composite was collected by centrifugation at 7000 rpm for 15 min. The obtained solid was dried in a vacuum oven at 60 °C for 12 h. The various concentrations of AGQD in composite were also prepared from 2.5, 5, 7.5, and 10 wt%, assigning P25-AGQD-2.5.

2.4. Characterizations

The nanostructures and morphology were observed with transmission electron microscopy (TEM) and high resolution TEM (HR-TEM) carried out using a JEOL, JEM-2100F transmission electron microscope. Topographic heights of the AGQDs deposited on a mica substrate were studied using taping mode of atomic force microscopy (AFM; Veeco, Dimension 3100). X-ray photoelectron spectroscopy (XPS; Thermo Fisher) measurements were performed using monochromatic AlKα radiation ($hv = 1486.6$ eV). XPS samples were prepared by drop casting 1 mL of AGQDs solution (0.5 mg/mL) on a SiO$_2$/Si substrate (300-nm-thickness SiO$_2$) and drying natually at room temperature. UV-visible absorption spectrum was derived from Specord 210 UV-vis spectrophotometer. Raman Spectroscopy was taken from 1000 to 2000 cm^{-1} at room temperature using a DXR Raman spectrometer with a 532 nm excitation source (Thermo Scientific). The Fourier transform infrared (FTIR) spectra were measured to determine the functional groups using a Nicolet IR 200 FT-IR spectrometer (Thermo Scientific) on sample pellets made with KBr. Fluorescence spectroscopy was taken at room temperature using a Cary Eclipse Fluorescence Spectrophotometer (GQDs in deionized water were excited at 440 nm).

2.5. Dyes photodegradation measurements

Typically, 50 mg of the catalyst was added into 50 mL of MB (methylene blue) solution (20 ppm) and stirred in the dark for 30 min. Then the solution was stirred and exposed to a 300 W xenon lamp with a 400 nm cut-off filter. After a specific time interval, 3 ml of the solution was taken and submitted to centrifugation to separate the catalyst. The MB concentration was recorded by the absorbance value at the strongest peak at 660 nm using a Specord 210 UV-vis spectrophotometer [20].

3. Results and discussion

Scheme. 1 illustrates the facile route to synthesize amine-functionalized GQDs by one-step carbonization of glucose in the presence of ammonia and H_2O_2 under microwave treatment. Glucose molecules play a role as carbon source for forming graphene framework. Otherwise, ammonia and H_2O_2 may contribute to the reaction functionalizing amine groups at the edges of GQDs. The as-prepared GQDs with functionalities have a high solubility and stability in aqueous media.

The TEM image of the AGQDs is presented in Fig. 1a. The obtained AGQDs can be observed as quasi-spherical and monodispersed particles with relatively uniform distribution, providing an average size of 3.78 nm ± 0.6 nm (inset of Fig. 1a). As shown in Fig. 1b, the high-resolution TEM (HRTEM) image reveals that the AGQDs consist of a high crystalline structure with an interplane spacing of 0.25 nm, responding to (1120) lattice fringes of graphene [21,22]. The topographic morphology and the heights of AGQDs are investigated by AFM measurement as shown in Fig. 1c and d. The heights of AGQDs are distributed primarily between 0.5–2 nm, with an average height of 1.3 nm ± 0.2 nm, which is close to the average thickness of 2–3 graphene layers.

The chemical structure of the functionalized GQDs was evaluated via FT-IR spectra and XPS. Fig.2a displays the FT-IR spectra of GQDs and AGQDs. The FT-IR spectrum of unfunctionalized GQDs exhibits abroad absorption peaks of the H-bonded associated −OH at around 3501 cm^{-1} and the peaks at 1431, 1625 cm^{-1}, and 1720 cm^{-1} correspond to the group of the deformation of C−O, in-plane vibration of sp^2-bonded carbon atoms, and the stretching vibration of C=O in the carboxyl group, respectively. In comparison, the FTIR spectrum of AGQDs presents two additional peaks

relating to functionalized amine. The band appears at 3146 cm^{-1}, which is ascribed to N−H bending vibration. The other peaks at 1352 cm^{-1} and 1620 cm^{-1} can be assigned to the C−N and N−H of primary amine bending vibration. These new bands indicate successful formation of an amine functional group on the surface of the GQDs. Furthermore, X-ray photoelectron spectroscopy (XPS) was performed to determine the chemical composition of the AGQDs. The survey XPS spectrum of AGQDs (Fig. 2b) displays clear signals of oxygen (O 1s ~532 eV), carbon (C 1s ~285 eV) peaks, as well as a pronounced nitrogen peak (N 1s ~400 eV). Additionally, the high-resolution C 1s XPS spectrum of AGQDs shows the C−C bond at 284.4 eV, C−N bond at 285.7 eV, the carbon hydroxyl groups (C−OH) at 286.6 eV, and carboxylate carbon group (O−C=O) at 288.7 eV (Fig. 2c). The presence of C−N bonding indicates the existence of N atoms in the quantum dots. To further identify the dominant type of bonding configuration of N atoms in AGQDs, N 1s XPS spectrum of AGQDs was studied as shown in Fig. 2d. The N 1s spectrum presents two group peaks at 399.3 and 401.2 eV, which can be assigned to amine band and protonated amine of the GQDs, respectively. Thus, the SPX results reveal that the primary amine group (NH_2) may be mainly formed during the hydrothermal reaction and have important contribution to optical properties of the functionalized GQDs. These results are also consistent with the corresponding FTIR spectroscopy results.

Fig. 3a presents the Raman spectroscopy of both pristine GQDs (black line) and AGQDs (red line). The unfunctionalized GQDs show two typical peaks assigned to the D peak (1356 cm^{-1}) and G peak (1591 cm^{-1}). As reported in the literature [23], the D band originates from disorder- or defects-related functionalities on surface of GQDs, while the G band is attributed to first-order scattering of Raman-active E_{2g} mode observed for C sp^2 atom in hexagonal lattice. Compared to the pristine GQDs, AGQDs exhibit a downshift of both G peak (11 cm^{-1}) and D peak (7 cm^{-1}). Additionally, the I_D/I_G ratio (1.12) of the functionalized GQDs is higher than that of the GQDs (0.99). These may be due to attachment of the primary amine group on GQDs, thus leading to generate more edges and defects during the functionalizing process. UV-vis absorption spectra of AGQDs (Fig. 3b) have an observable two absorption peak located at about 322 nm and 442 nm which are attributed electron transition from $\pi \rightarrow \pi^*$ of the aromatic sp^2 domain and $n \rightarrow \pi$ of amine group at the edges of GQDs. In comparison to the pristine GQDs, the functionalized GQDs
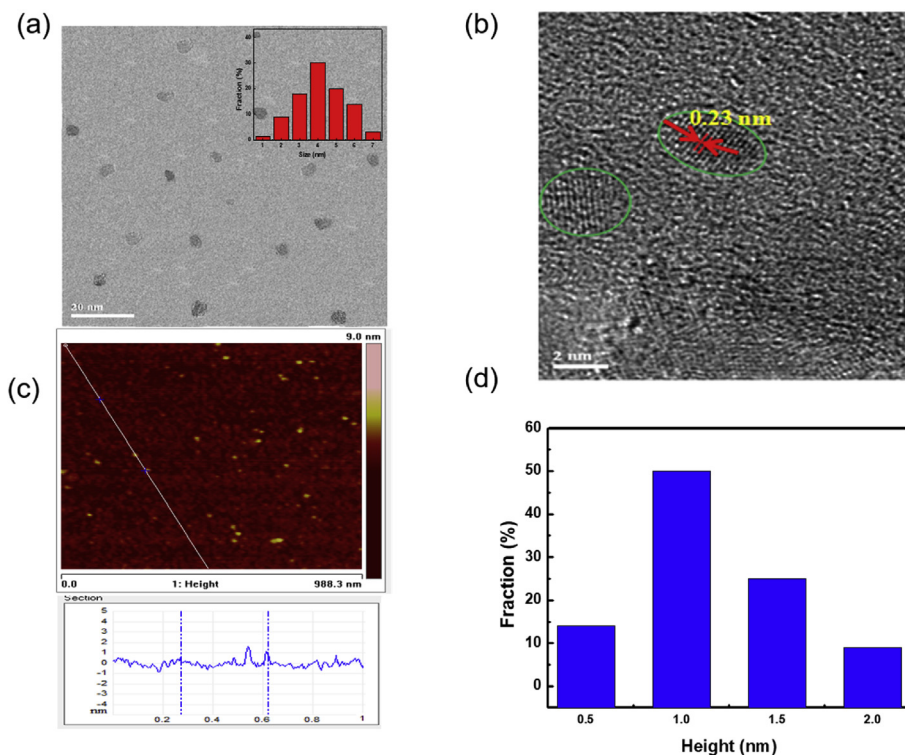

Scheme 1. Synthesis of AGQDs.
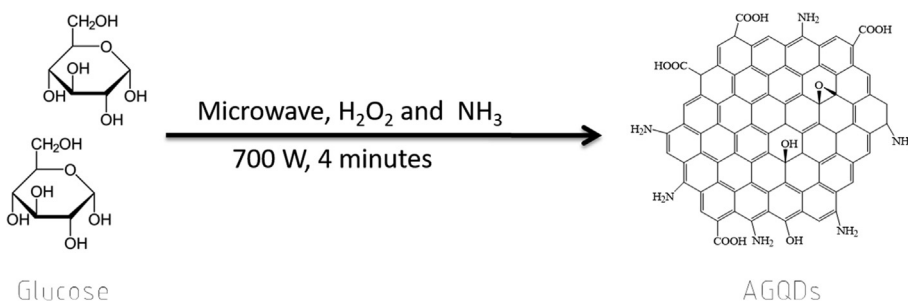
Fig. 1. (a,b) TEM and HRTEM images of AGQDs, respectively. The inset in (a) shows the size distributions of AGQDs. (c,d) AFM image and height distributions of the GQDs.

exhibit a blue shift by about 50 nm which may result from amino functionalization, altering electron band transition.

To further explore optical property, the investigation of emission spectra for amine-functionalized GQDs is illustrated in Fig. 4 by using fluorescent spectroscopy. It is found that the fluorescent spectra of AGQDs have emission peaked at around 500 nm (Fig. 4a), which is an 80 nm shift toward longer emission wavelength, as compared to unfunctionalized GQDs (420 nm). It is clearly observed that the AGQDs exhibit a green fluorescence color taken under irradiation by a 365 nm lamp (20 W) (Fig. S1). Interestingly, the AGQDs possess wide range absorption from 400 to 550 nm, which is beneficial for a visible-light photocatalyst. As reported previously, a functional group covalently bonded on the graphene quantum dots can lead to changes in the surface state, which causes modification of the electronic structure. For amino-contained GQDs, $-NH_2$ groups may be attributed to creating additional energy levels within band structure because of strong orbital interaction between delocalized π orbital in the conjugated structure and molecule orbital in amine moieties [24]. It results in reduction of optical band gap of the GQDs, thus leading to a redshift in fluorescence spectra. This tunable fluorescent emission of GQDs has been reported in both experimental observations and quantum-mechanical calculations. The value of quantum yield of the AGQDs was determined to be about 39% using quinine sulfate as the reference. Moreover, the excitation wavelength dependence of AGQDs is clearly observed in Fig. 4b. When the excitation wavelength is increased from 300 to 500 nm, the emission peaks of

AGQDs vary in a wide range from 460 nm to 550 nm. When excited by longer wavelengths from 300 to 440 nm, the position of the peak is shifted to longer wavelengths with increment of the intensity. The emission peak remains redshifted with intensity decreased gradually, when excited from 460 to 500 nm. At an excitation wavelength of 440 nm, the fluorescence spectra of amine-functionalized GQDs exhibit the most intense peak at about 500 nm. All these luminescent characteristics of as-prepared functionalized GQDs promise potential applications in sensing, bioimaging, and photocatalyst.

To further study the enhanced photocatalytic performance of AGQDs, a composite of the quantum dots and commercial TiO_2 (P25) was prepared and tested for degradation efficiency of methylene blue (MB) in the visible light region (>400 nm). After preparation, the color of TiO_2 changed from white to yellow (Fig. S2), indicating absorption of AGQDs on the surface of TiO_2 which responded to electrostatic interaction between amine group (positive charge) and OH groups (negative charge) on the TiO_2 surface. Fig. 5a presents the relation between MB normalized concentration (C/C_0) and irradiation time of various catalysts. Pure TiO_2 and AGQDs show very low photocatalytic activity with only 5% and 8% of the MB degraded after 120 min. On the other hand, by compounding TiO_2 and different concentrations of AGQDs, significantly enhanced dye photodegradation was observed. The composite with 7.5 wt% exhibits the highest visible-light photocatalytic efficiency that is approximately 85.3% and around 17 times higher than that of the
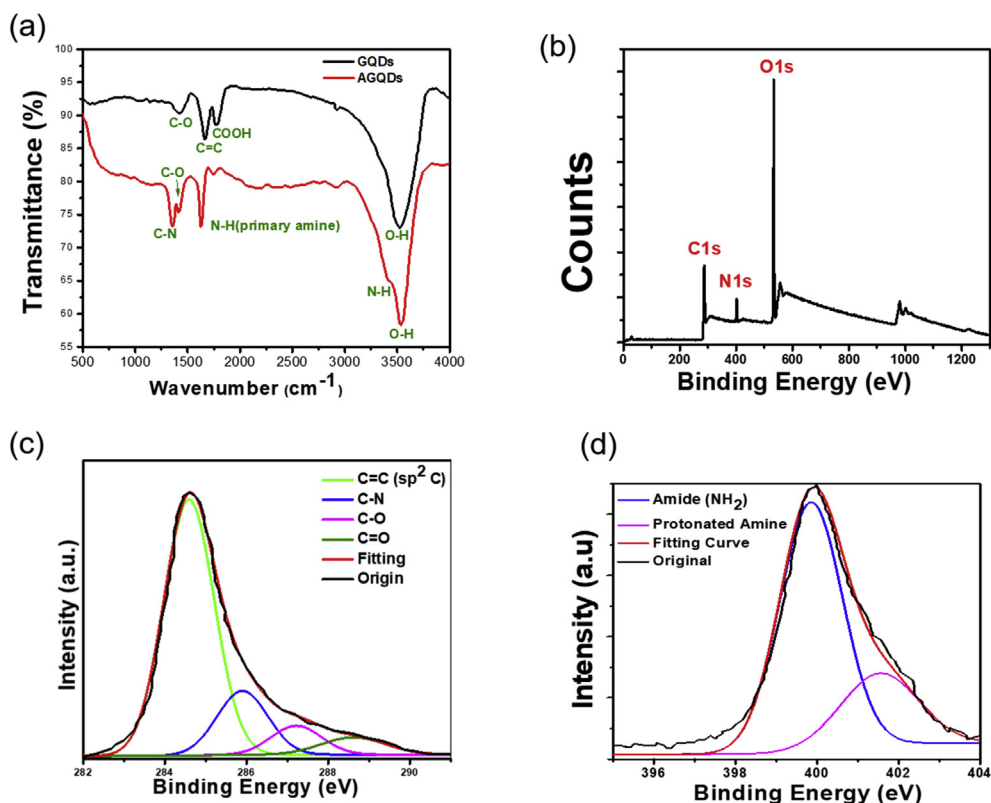
Fig. 2. (a) FTIR spectroscopy of the AGQDs. (b) XPS survey scan of as-obtained AGQDs. Specifications of C1s (c) and N1s (d).

commercial TiO_2. As shown in Fig. 5b, the rate reaction constant of P25-AGQDs 7.5 also perform excellent apparent rate. The cycle test was also performed to examine the stability of the composites. As shown in Fig. 5c, a slight change is observed in the photodegradation efficiency after five continuous measurements under visible light, indicating that our composite possess an outstanding photocatalytic stability for waste water treatment. Based on all of the above evidence, it can be explained that the superior photocatalyic activity of the composite can be attributed to

the integration of TiO_2 served as catalytically active site and AGQDs functioned as visible-light-irradiation-absorption regions which produce electron−hole pair and inject photogenerated electron into TiO_2. Fig. 5d illustrates the possible mechanism of MB photodegradation. Under visible light, electrons of AGQDs are excited from valance band to conducting band, thus generating electron−hole pairs. The photo-induced electrons are then rapidly transferred to TiO_2 which is attributed to the higher LUMO level of AGQD (LUMO = −4.26, HUMO = −7.46) than that of TiO_2
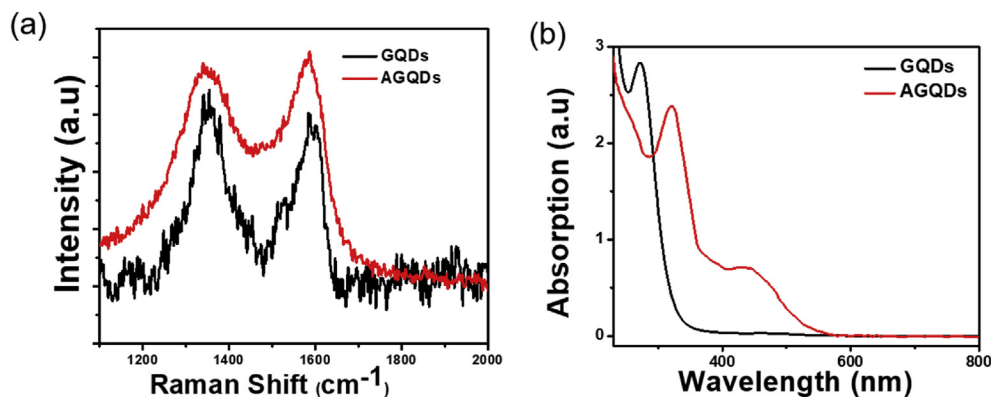

Fig. 3. (a) Raman spectroscopy of the AGQDs. (b)UV-vis absorption spectroscopy of as-produced AGQDs.
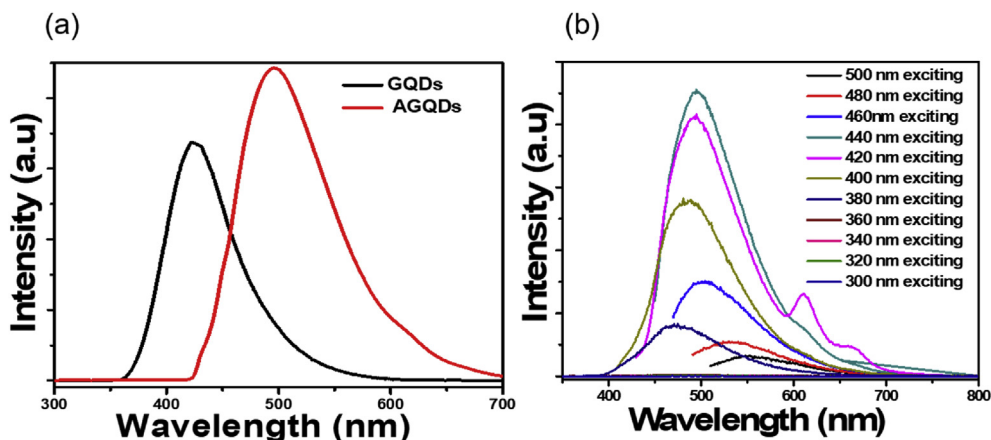
Fig. 4. (a) Photoluminescence spectra of GQDs and AGQDs. (b) The fluorescence speactra of the AGQDs at different excitation wavelengths ranging from 300 nm to 500 nm.
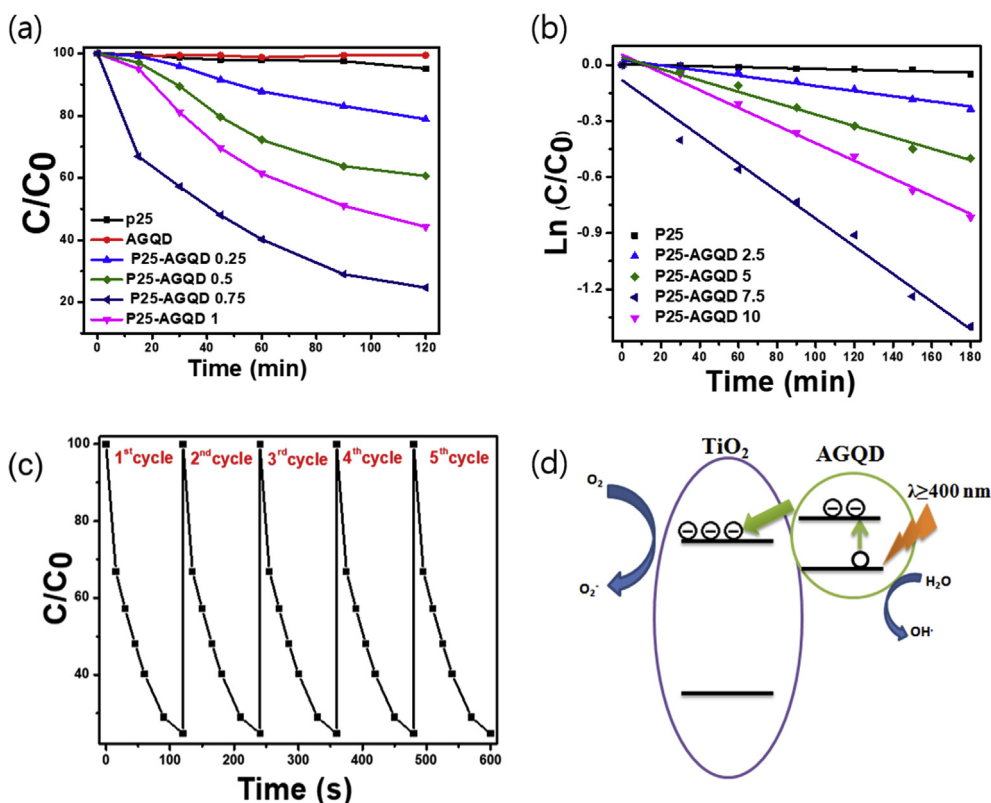

Fig. 5. (a) Photocatalytic degradation of MB solution by P25 and TiO₂/AGQD composites with different amounts of GQDs under visible light. (b) Kinetic studies of the TiO₂/AGQD composites for MB degradation under visible light. (c) Cycling curve of photodegradation of the composites (P25-AGQDs 0.75). (d) Schematic diagram of photogenerated electron transfer between AGQDs and TiO₂.

(LUMO = −3.97, HUMO = −5.91) [25,26]. The electron in the conducting band of TiO_2 reacts with oxygen to form oxygen active, while the hole in the LUMO level of AGQD reacts with water to produce radical hydroxyl (˙OH). The MB molecules adsorbed on the TiO_2 surface can be oxidized by strong oxidation of $O_2^{˙}$ radical, thus leading to effective degradation of MB.

4. Conclusion

We have developed a simple synthesis procedure for AGQDs from the carbonization of glucose through hydrothermal treatment in the presence of ammonia and H_2O_2. These synthesized AGQDs were mainly composed of 2−3 layers with a uniform size of about 4.34 nm. The AGQDs

also show bright green luminescence with a higher PL quantum yield of 39%. Furthermore, we have demonstrated the high visible light photocatalytic activity of the composite of TiO_2 and AGQDs for effective dye photodegradation. The enhanced performance is response for high visible light absorption and rapid transferring of photo-induced charge carriers to the suface of AGQDs. Our approach may open a new way to develop a green, inexpensive, and convenient method for large-scale production of novel photcatalyst hybrid materials in treatment of waste water.

Appendix A. Supplementary data

Supplementary data to this article can be found online at https://doi.org/10.1016/j.crci.2019.10.005.

References

[1] X.L. Li, X.R. Wang, L. Zhang, S.W. Lee, H.G. Dai, Chemically derived, ultrasmooth graphene nanoribbon semiconductors, Science 319 (2008) 1229–1232.

[2] L.A. Ponomarenko, F. Schedin, M.I. Katsnelson, R. Yang, E.W. Hill, K.S. Novoselov, A.K. Geim, Chaotic dirac billiard in graphene quantum dots, Science 320 (2008) 356–358.

[3] X. Xu, R. Ray, Y. Gu, H.J. Ploehn, L. Gearheart, K. Raker, W.A. Scrivens, Electrophoretic analysis and purification of fluorescent single-walled carbon nanotube fragments, J.Am. Chem. Soc. 126 (2004) 12736–12737.

[4] S.Y. Ju, W.P. Kopcha, F. Papadimitrakopoulos, Science 323 (2009) 1319–1323.

[5] S.J. Yu, M.W. Kang, H.C. Chang, K.M. Chen, Y.C. Yu, Bright fluorescent nanodiamonds: No photobleaching and low cytotoxicity, J. Am. Chem. Soc. 127 (2005) 17604–17605.

[6] S.N. Baker, G.A. Baker, Luminescent carbon nanodots: Emergent nanolights, Angew. Chemie.Chem.Int. Ed. 49 (2010) 6726–6744.

[7] Y. Li, Y. Hu, Y. Zhao, G. Shi, Q.L. Deng, Y.B. Hou, L.T. Qu, An electrochemical avenue to green-luminescent graphene quantum dots as potential electron-acceptors for photovoltaics, Adv. Mater. 23 (2011) 776–780.

[8] X. Sun, Z. Liu, K. Welsher, J.T. Robinson, A. Goodwin, S. Zaric, H. Dai, Nano-graphene oxide for cellular imaging and drug delivery, NanoRes 1 (2008) 203–212.

[9] J. Shen, Y. Zhu, X.L. Yang, C.Z. Li, Graphene quantum dots: Emergent nanolights for bioimaging, sensors, catalysis and photovoltaic devices, Chem. Commun. 48 (2012) 3686–3899.

[10] J.H. Shen, Y.H. Zhu, X. Yang, J. Zong, J.M. Zhang, C.Z. Li, One-pot hydrothermal synthesis of graphene quantum dots surface-passivated by polyethylene glycol and their photoelectric conversion under near-infrared light, New J. Chem. 36 (2012) 97–101.

[11] D.Y. Pan, J.C. Zhang, Z. Li, M.H. Wu, Hydrothermal route for cutting graphene sheets into blue-luminescent graphene quantum dots, Adv. Mater. 22 (2010) 734–738.

[12] J.H. Shen, Y.H. Zhu, C. Chen, X.L. Yang, C.Z. Li, Facile preparation and upconversion luminescence of graphene quantum dots, Chem. Commun. 47 (2011) 2580–2582.

[13] X. Yan, X. Cui, Large, solution-processable graphene quantum dots as light absorbers for photovoltaics, Nano Lett 10 (2010) 1869–1973.

[14] R. Liu, D. Wu, X. Feng, K. Mullen, Bottom–up fabrication of photoluminescent graphene quantum dots with uniform morphology, J. Am. Chem. Soc. 133 (2011) 15221–15223.

[15] X. Chen, S.S. Mao, Titanium dioxide nanomaterials: synthesis, properties, modifications, and applications, Chem Rev107 (2007) 2891–2959.

[16] T. Morikawa Asahi, T. Ohwaki, K. Aoki, Y. Taga, Visible-light photocatalysis innitrogen-doped titanium oxides, Science 293 (2001) 269–271.

[17] K. Mori, M. Kawashima, H. Yamashita, Visible-light-enhanced Suzuki-Miyauracoupling reaction by cooperative photocatalysis with an Ru-Pd bimetallic complex, Chem. Commun. 50 (2014) 14501–14503.

[18] P. Wang, J. Wang, T. Ming, X. Wang, H. Yu, J. Yu, Y. Wang, M. Lei, Dye-sensitization-induced visible-light reduction of graphene oxide for the enhanced TiO_2 photocatalytic performance, ACS Appl. Mater. Inter. 5 (2013) 2924–2929.

[19] T.V. Tam, W.M. Choi, One-pot synthesis of highly fluorescent amimo-functionalized graphene quantum dots for effective detection of copper ions, Curr. Appl. Phys. 18 (2018) 1255–1260.

[20] H.N. Tien, V.H. Luan, L.T. Hoa, N.T. Khoa, S.H. Hahn, J.S. Chung, E.W. Shin, S.H. Hur, One-pot synthesis of a reduced graphene oxide-zinc oxide sphere composite and its use as a visible light photocatalyst, Chem. Eng. 229 (2013) 126–133.

[21] J. Peng, W. Gao, B.K. Gupta, Z. Liu, R. Romero-Aburto, L. Ge, L. Song, L.B. Alemany, X. Zhan, G. Gao, S.A. Vithayathil, B.A. Kaipparettu, A.A. Marti, T. Hayashi, J.J. Zhu, P.M. Ajayan, Graphene quantum dots derived from carbon fibers, Nano Lett. 12 (2012) 844–849.

[22] X. Dong, D. Fu, W. Fang, Y. Shi, P. Chen, L.J. Li, Doping single-layer graphene with aromatic molecules, Small 5 (2009) 1422–1426.

[23] Z. Wang, H. Zeng, L. Sun, Graphene quantum dots: versatile photoluminescence for energy, biomedical, and environmental application, J. Mater. Chem. C 3 (2015) 1157–1165.

[24] H. Tetsuka, H. Tetsuka, R. Asahi, A. Nagoya, K. Okamoto, I. Tajima, R. Ohta, A. Okamoto, Optically tunable amino-functionalized graphene quantum dots, Adv. Mater. 24 (2012) 5333–5338.

[25] H. Tetsuka, A. Nagoya, T. Fukusumi, T. Matsui, Molecularly designed, nitrogen-functionalized graphene quantum dots for optoelectronic devices, Adv. Mater. 28 (2016) 4632–4638.

[26] E. Regulska, D.M. Rivera-Nazario, J. Karpinska, M.E. Plonska-Brzenzinska, L. Echegoyen, Zinc pohyrin-functionalized fullerenes for the sensitization of titania as a visible-light active photocatalyst: river waters and wastewaters remediation, Molecules 24 (1) (2019) 1118, 1118.